1

Introduction to Proton Exchange Membrane Fuel Cells

1.1 Overview of Proton Exchange Membrane Fuel Cells Technology

Proton exchange membrane fuel cells (PEMFCs) are at the forefront of clean energy innovation, offering a sustainable and efficient means of power generation that is pivotal in addressing the challenges of global energy demands and environmental sustainability. PEMFCs work by converting the chemical energy of hydrogen directly into electrical energy through an electrochemical process, with water and heat as the only by-products. PEMFCs have widespread attention among clean energy technologies, renowned for their high efficiency, low operating temperatures, and rapid start-up times, making them suitable for a wide range of applications, from automotive and stationary power generation to portable power devices [1, 2]. As the world increasingly shifts toward renewable energy sources, PEMFCs provide a compelling alternative to traditional fossil fuel–based energy systems. Their ability to generate power with zero-greenhouse-gas emissions makes them an essential component in the global efforts to combat climate change and reduce the carbon footprint of energy production.

1.1.1 Brief History and Development of Proton Exchange Membrane Fuel Cell

The concept of fuel cells dates back to the nineteenth century when Sir William Grove first demonstrated the "gaseous voltaic battery" in 1839. However, it wasn't until the mid-twentieth century that significant advancements were made in fuel cell technology, primarily driven by the need for efficient power sources in space missions. While PEMFCs are a distinct type of fuel cell, their development is intrinsically linked to hydrogen as the primary fuel source. The exploration of hydrogen as a clean energy carrier has paralleled the advancement of PEMFC technology [3]. This synergy is crucial for the widespread adoption of fuel cell technologies, as hydrogen provides the necessary energy source that powers PEMFC systems. However H_2 as a low-carbon-energy system is not new; the wave of enthusiasm

Electrospinning for Proton Exchange Membrane Fuel Cells, First Edition.
Yong Liu and Mohideen Meerasahib Mohamedazeem.

for hydrogen began in the early 1970s due to the first global energy demand and environmental crisis; thus, many hydrogen energy-based research programs were launched. For instance, the International Energy Agency (IEA) was established in 1974, the *International Journal of Hydrogen Energy* launched in 1976, and the IEA Hydrogen and Fuel-Cell Technology Collaboration Programme in 1977. Since then, a growing number of researchers, international organizations, and companies have supported the hydrogen-based economy to address the fossil fuel demand and control greenhouse gas (GHG) emissions [4]. The historical key milestone of hydrogen and fuel cells is depicted in Figure 1.1.

Today, hydrogen and fuel cell technologies offer a promising path toward sustainable energy. Ongoing research and development aim to overcome current challenges, such as reducing the reliance on precious metals and improving system efficiency and durability. Continued investment in research and infrastructure is essential to realizing the full potential of hydrogen as a clean energy carrier. Moreover, hydrogen is a versatile energy carrier, not an energy source, having potential applications to provide energy services across all sectors: transportation, power, building, and industry. Hydrogen is itself a carbon-free carrier, but a significant amount of carbon footprint occurs during its production [1, 4]. Presently, hydrogen is produced from various primary energy sources such as fossil fuels, biomass, and renewables. Low-carbon technological options like carbon capture and storage (CCS) and electrolyzers require extensive development to reduce carbon dioxide (CO_2) emissions during hydrogen production. As an energy carrier, hydrogen can overcome the variable renewable energy flexibility issue on the energy supply-and-demand side by enabling the linkage between them by connecting various transmission and distribution networks [5]. Hydrogen and fuel cell technologies are an excellent solution to decarbonize the transport sector. Green hydrogen produced from renewable energy sources such as solar photovoltaic (PV) and wind power could be integrated into fuel cell vehicles as a promising alternative to internal combustion engines [1, 5].

1.1.2 Need for H_2-Powered Fuel Cell Technology in Today's World

In the face of addressing global environmental challenges and an urgent need for sustainable energy solutions, hydrogen-powered fuel cell technology has emerged as a critical component in the global energy transition. The pressing issues of climate change, air pollution, and energy security have highlighted the necessity of moving away from fossil fuel dependency and toward cleaner, renewable energy sources [6]. The transport sector is one of the fast-growing and key driving forces of anthropogenic environmental pressure, contributing nearly 20% of GHG emissions, with fossil fuels accounting for almost 90% of total energy consumption. One-quarter of all energy-related GHG emissions are related to transportation, with around 72% of these overall emissions generated from road transport. Recently, the COVID-19 pandemic decreased global transport emissions by 10%, or 7.2

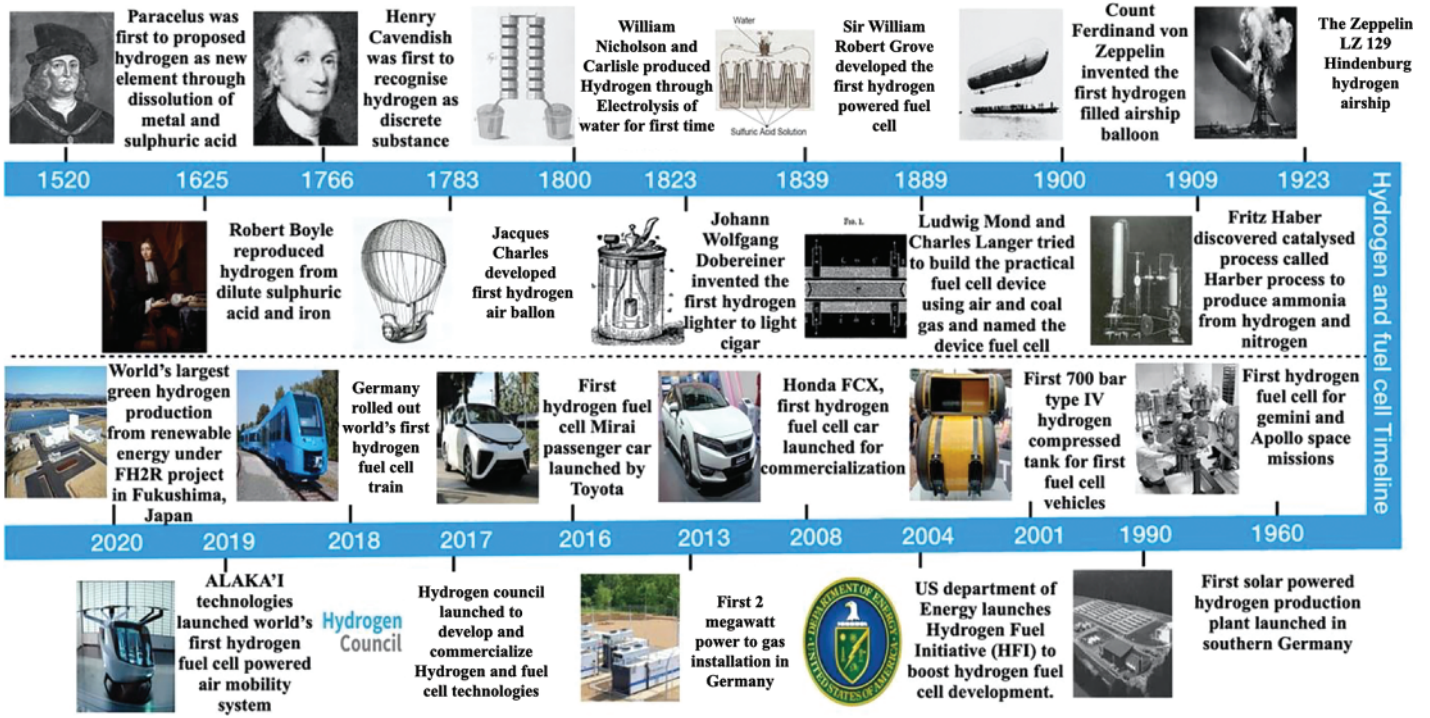

Figure 1.1 Hydrogen and fuel cell technology timeline. Source: Mohideen et al. [4]/with permission of Elsevier.

gigatonne (Gt) of carbon dioxide (CO_2) in 2020, compared to 8.5 Gt of CO_2 in 2019, due to the pandemic-related restrictions on domestic and international travel. However, in 2022, the CO_2 emissions associated with the transport sector began to rebound with the lifting of travel restrictions around the world [1, 4].

Today, a well-to-wheel passenger vehicle generates an average of 300 g of CO_2 per kilometer. According to the IEA, achieving a net-zero-emission transport sector requires a further drop in carbon emissions by 20% to 5.7 Gt by 2030 from the current level. Achieving such a drastic emission drop highly depends on the policies driving the revolutionary shift from fossil-fuel-based vehicles to clean and green mobility. Today, several low-carbon road transport technologies are readily available in the market, including plug-in hybrid vehicles, battery electric vehicles, and fuel cell electric vehicles (FCEVs). However, all these technologies are at various commercialization phases, and the significance of each in the sustainable future transport sector is a topic of discussion. Hydrogen-powered FCEV has the potential to decarbonize the transport sector compared to other low-carbon transport technologies. The proton exchange membrane (PEM) fuel cell stack is mostly used in FCEVs, offering high power density, high efficiency, and cold-start capabilities. In addition, hydrogen-powered FCEVs have widespread advantages, including high range and short refueling time (~500 km and 3 min), high well-to-wheel efficiency, smooth operation (low noise), and quick start-up. Owing to such overwhelming benefits, hydrogen-powered FCEVs will be a competitive edge in future transportation, especially for heavy-duty vehicles, trucks, buses, maritime shipping, and aviation sectors. However, compared to gasoline-powered and electric-powered vehicles, the number of FCEVs on the road is comparatively small, due to its high production cost of materials and infrastructure.

On the road to net-zero-emission scenario, it is anticipated that the hydrogen demand will reach almost 2.6% of the total transport sector energy demand by 2030 and over one-quarter by 2050. Nevertheless, in the current scenario, the use of hydrogen in the transport sector is much lower than that in other sectors, accounting for <0.01% of the energy consumed. For instance, if all the 1 billion cars, 25 million buses, and 190 million trucks on the road are replaced by FCEVs in the future, then the demand for global green hydrogen will be fourfold higher than the current level. From 2017 to 2020, the global share of FCEVs stock skyrocketed by an annual average of 70%, and as of June 2021, more than 40,000 FCEVs were on the road, mostly in the United States and Japan. The United States accounts for the second largest FCEV fleet, with more than 9,200 vehicles sold at the end of 2020. Japan presently has 4100 FCEVs on the road and is targeted to manufacture 800,000 passenger light-duty vehicles (PLDVs) by 2030. It was followed by Korea, which took the lead in the FCEVs market between 2019 and 2020, and by the end of June 2020 alone, 4400 PLDVs had been registered, and the government targeted 200,000 and 2.9 million light-duty FCEVs by 2025 and 2040, respectively.

Although FCEVs hold tremendous advantages in decarbonization transport sector, the cost of fuel cell components is a key barrier that hinders the widespread commercialization of FCEVs. For instance, the high cost of

Table 1.1 Approximate cost of platinum content in PEMFC vehicles based on current target platinum loading.

Stack power (kW)	Application	Example	Total Pt (g)	Total cost of Pt (USD)
1–25	Portable power and scooters		0.3–8	10–240
25–75	Range extenders, buses, and trucks		8–25	240–750
>75	Passenger vehicles		25–35	750–1050

Source: Banham et al. [7]/Elsevier/CC BY 4.0.

the expensive platinum metal used as a cathode catalyst in a fuel cell stack itself is responsible for 56% of its total cost of ownership. As shown in Table 1.1, for mid-sized passenger FCEVs, 25–35 g of Pt is required, which is 10-fold higher than a diesel autocatalyst. Therefore, reducing the platinum loading of the catalyst in the fuel cell stack is critical for the economic viability of FCEVs. In this direction, Daimler has significantly reduced platinum usage in their FCEVs by nearly 90% of platinum by ~8 g to just 5 g per vehicle [8]. Similarly, Toyota's Mirai FCEV cuts platinum utilization by 50% through alloying with cobalt (Pt/Co), an approach that plays.

In this context, electrospun nanofibers, prepared via the electrospinning technique, have garnered considerable attention to reduce the cost of the key components as well as improve the performance of fuel cell. The concept of electrospinning experienced a resurgence in the 1990s as nanomaterials became a research priority. The technique has since found diverse applications in biotechnology, filtration, energy storage, medicine, aerospace, and electronics [9]. As illustrated in Figure 1.2, a typical electrospinning setup includes a high-voltage power supply, a spinning apparatus (composed of a feed pump and syringe), and a collector. The process involves generating a strong electrostatic field between the spinning apparatus and the collector. When the electrostatic force acting on the polymer solution overcomes its surface tension and viscosity, a charged jet forms at the apex of the Taylor cone. This jet stretches, undergoes solvent evaporation and solidification, and finally deposits on the collector as nanofibers. The resulting fiber diameters typically range from tens of nanometers to several microns [11].

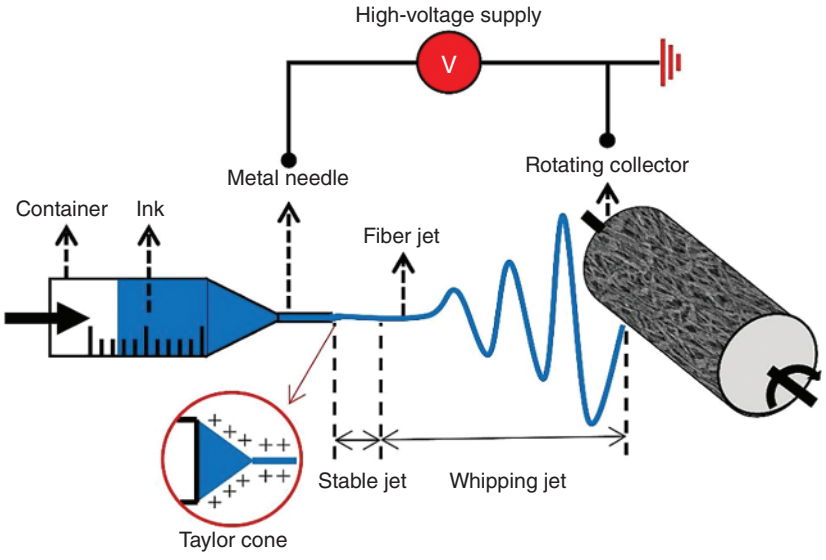

Figure 1.2 Schematic diagram of electrospinning device. Source: Yong et al. [10]/with permission of Elsevier.

1.2 Key Components of Proton Exchange Membrane Fuel Cell

PEMFCs are complex systems that rely on the seamless integration of several critical components to convert hydrogen into electrical energy efficiently. Each component plays a vital role in ensuring the effective operation of the fuel cell, with maximum efficiency and durability. A deeper understanding of these components is crucial for advancing PEMFC technology and optimizing its performance across various applications. The core components of a PEMFC include the PEM, catalyst layer (CL), gas diffusion layer (GDL), bipolar plates, and the flow field. Together, these elements form a cohesive system that facilitates the electrochemical reactions necessary for power generation in FCEVs, as illustrated in Figure 1.3.

1.2.1 Catalyst Layer

The CL is typically a thin, porous structure consisting of catalyst particles, an ionomer, and a carbon support. The platinum or platinum alloy catalyst particles are dispersed on a high-surface-area carbon support to maximize the available catalytic surface area. The ionomer, often Nafion, is interspersed throughout the layer to aid proton conduction and ensure effective contact with the membrane [12–15]. The primary function of the CL is to accelerate the electrochemical reactions within the fuel cell, ensuring efficient conversion of hydrogen and oxygen into water and electrical energy. The efficiency and performance of the PEMFC are heavily dependent on the activity and stability of the CL. The catalysts must exhibit high

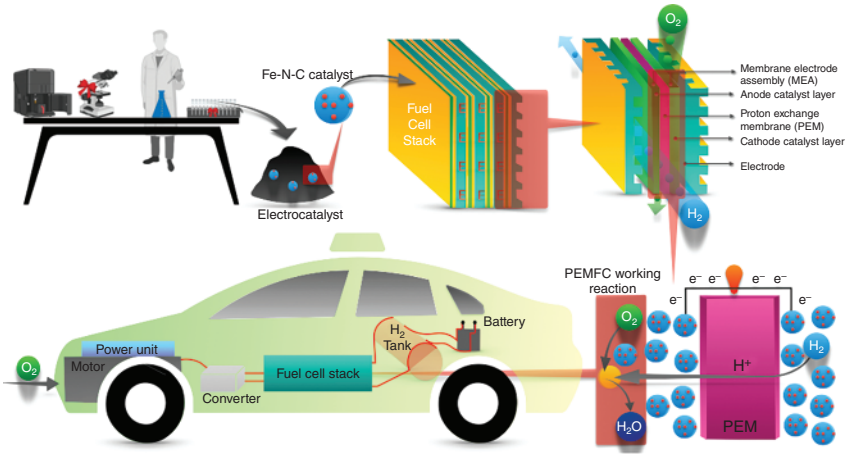

Figure 1.3 Schematic illustration of key components in FCEVs. Source: Mohideen et al. [8]/with permission of Elsevier.

catalytic activity to facilitate fast reaction rates while maintaining stability under the operating conditions of the fuel cell [16].

The thickness of the CL is a crucial factor influencing its performance. Thicker CLs provide a higher total catalytic surface area per geometric area, which can enhance performance by increasing reaction rates. However, they also introduce higher resistance to the transport of electrons, protons, reactants, and products, potentially negatively affecting overall fuel cell performance [17–19]. This trade-off between surface area and transport resistance necessitates careful optimization of the CL thickness. The porosity of the CL is approximately 30%, with a hierarchical pore structure that includes primary pores less than 10 nm and secondary pores less than 100 nm. This porosity facilitates the effective transport of reactants and products, as well as the distribution of gases across the catalyst surface. Achieving the optimal balance of porosity and pore size is critical for maintaining efficient mass transport and minimizing diffusion losses [20].

At the CL, two critical electrochemical reactions occur that convert chemical energy into electrical energy:

(i) **Hydrogen Oxidation Reaction (HOR)**: At the anode, hydrogen molecules (H_2) are split into protons (H^+) and electrons (e^-) by the catalyst. The protons migrate through the PEM, whereas the electrons are directed through an external circuit, providing electric power. HOR reaction can be represented by the following equation:

$$H_2 \rightarrow 2H^+ + 2e^-$$

(ii) **Oxygen Reduction Reaction (ORR)**: ORR occurs at the cathode of the PEMFC, where oxygen molecules are reduced to form water. The ORR kinetics at the cathode is slower than that at the anode even though the Pt catalyst loading at the cathode was 10 times higher than those at the anode. The reason for

sluggishness and high catalyst loading of the cathode is the grand challenges of ORR, namely, that (i) the cathode catalyst should withstand extreme corrosive circumstances and eventually be chemically active enough to activate O_2, (ii) it should be noble enough to facilitate the facile release of by-product water at the end of the reactions from the surface of the catalyst, and, (iii) as a consequence, ORR at the cathode is responsible for half of the voltage loss in the PEMFC system, whereas the voltage loss of HOR is considerably small even with a very low Pt loading of 0.05 mg/cm^2. As a consequence, the high loading of Pt accounts more than half of the total cost of the fuel cell [8].

ORR is the most prominent reaction in PEMFCs and alkaline membrane exchange fuel cells, involving a series of electron transfer steps by undergoing electrochemical reduction of O_2 molecules in an acidic or alkaline electrolyte. The general ORR catalytic reactions are either a four-electron pathway ($4e^-$) or a two-step, two-electron ($2e^-$) pathway, as shown in the following equations:

(i) The direct $4e^-$ pathway: It is a universally accepted reaction process that directly reduces the O_2 molecules to H_2O in acid media, and to OH^- in alkaline media.
$4e^-$ pathway in acid medium:

$$O_2 + 4H^+ + 4e^- \rightarrow 2H_2O$$

$4e^-$ pathway in alkaline medium:

$$O_2 + 2H_2O + 4e^- \rightarrow 4OH^-$$

(ii) The two-step, two-electron ($2e^-$) pathway: The reaction process includes a series of steps by producing H_2O_2 and then reduce to H_2O.
$2e^-$ pathway in acid medium:

$$O_2 + 2H^+ + 2e^- \rightarrow H_2O_2$$

$$H_2O_2 + 2H^+ + 2e^- \rightarrow 2H_2O$$

$2e^-$ pathway in alkaline medium:

$$O_2 + H_2O + 2e^- \rightarrow HO_2^- + OH^-$$

$$HO_2^- + H_2O + 2e^- \rightarrow 3OH^-$$

However, in the $4e^-$ pathway, two types of possible reaction kinetics were proposed, such as the dissociative and associative reaction pathways, as shown in Table 1.2.

It is essential to note that the dissociating energy barrier of the initial O_2 adsorption molecule plays a crucial role in deciding whether the catalyst undergoes an associative or dissociative pathway. However, due to the high O_2 dissociation barriers on metal-N_x moieties, the associative mechanism is more suitable for nonprecious metal catalysts in both acidic and alkaline environments [21]. Both mechanisms involve various intermediate species during the reaction pathways, including hydroxyl (OH^*), oxygenated (O^*), and super hydroxyl (OOH^*), and their corresponding transformations during the reaction make the ORR mechanism more complicated. Initially, O_2 molecule adsorption takes place, followed by weakening of the O–O bond and cleaving it to form two atomic O_2^* species that leads to the direct formation of OH^- without generating OOH^- [22–25].

Table 1.2 Associative and dissociative mechanisms of ORR in acid and alkaline electrolytes.

Acid	Alkaline
$4e^-$ associative mechanism	$4e^-$ associative mechanism
$O_2(g) + H^+ + e^- + {}^* \rightarrow OOH^*$	$O_2(g) + H_2O + e^- + {}^* \rightarrow OOH^* + OH^-$
$OOH^* + H^+ + e^- \rightarrow O^* + H_2O$	$OOH^* + e^- \rightarrow O^* + OH^-$
$O^* + H^+ + e^- \rightarrow OH^*$	$O^* + H_2O + e^- \rightarrow OH^* + OH^-$
$OH^* + H^+ + e^- \rightarrow {}^* + H_2O$	$OH^* + e^- \rightarrow {}^* + OH^-$
$4e^-$ dissociative mechanism	$4e^-$ dissociative mechanism
$O_2(g) + {}^* \rightarrow O_2{}^*$	$O_2(g) + {}^* \rightarrow O_2{}^*$
$O_2{}^* \rightarrow O^* + O^*$	$O_2{}^* \rightarrow O^* + O^*$
$O^* + H^+ + e^- \rightarrow OH^*$	$O^* + H_2O + e^- \rightarrow OH^* + OH^-$
$OH^* + H^+ + e^- \rightarrow H_2O + {}^*$	$OH^* + e^- \rightarrow {}^* + OH^-$
$2e^-$ associative mechanism	$2e^-$ associative mechanism
$O_2(g) + H_+ + e^- + {}^* \rightarrow OOH^*$	$O_2(g) + H_2O + e^- + {}^* \rightarrow OOH^* + OH^-$
$OOH^* + H^+ + e^- + {}^* \rightarrow H_2O_2 + {}^*$	$OOH^* + e^- \rightarrow HO_2^- + {}^*$

Concerning the above-mentioned ORR mechanisms, it is clear that the performance of the ORR pathway depends on the nature of the electrocatalyst and electrolyte. Therefore, to reduce Pt usage without compromising the stability, durability, and ORR performance of fuel cell [26], the appropriate electrocatalysts can be developed using the following strategies: (i) alloying Pt with other transition metal, (ii) replacing Pt with nonprecious transition metals, and (iii) metal-free carbon-based electrocatalyst.

1.2.2 Gas Diffusion Layer

GDL is a vital component of PEMFCs, ensuring effective transport of gases and water between the CL and the flow field channels. Situated between the CL and the bipolar plates, the GDL facilitates uniform reactant distribution, provides electrical conductivity, and optimizes water management—factors essential for reliable fuel cell operation (Figure 1.4) [27–30].

Typically made from porous carbon materials such as carbon paper or carbon cloth, the GDL offers high permeability and excellent electrical conductivity. Carbon cloth, being more porous and less tortuous than carbon paper, exhibits greater compressibility. However, its higher compressibility can cause material to intrude into flow field channels, leading to uneven gas flow and performance variations [31, 32]. In contrast, carbon fiber paper is often preferred to the macroporous layer due to its superior mechanical strength. Its natural brittleness ensures higher compressive strength, supporting uniform gas flow and stable mechanical integrity within the fuel cell.

Water management is a critical function of the GDL, as it must maintain the membrane's hydration while preventing flooding at the CL. Effective water handling is key to achieving both high performance and long-term durability [33]. To this end,

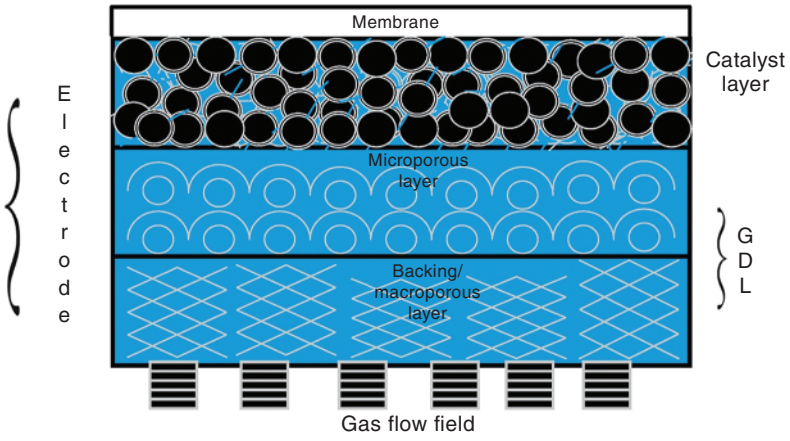

Figure 1.4 Schematic illustration of GDL.

GDLs are frequently treated with hydrophobic coatings—commonly polytetrafluoroethylene (PTFE)—to enhance water removal and prevent water accumulation. The GDL's porous structure not only facilitates the diffusion of hydrogen and oxygen to the CL but also aids in removing water vapor and any excess liquid water. Properly optimized porosity is essential to strike a balance between efficient gas transport and effective water management [34].

The thickness of the GDL typically falls within the range of 200–400 μm. While a thicker GDL can improve mechanical support and enhance water management, it can also increase resistance to gas diffusion. Thus, achieving the right balance of thickness and porosity is crucial for maximizing PEMFC performance [35].

1.2.3 Proton Exchange Membrane

The PEM is the core component of a PEMFC, serving as the electrolyte that facilitates proton transport while preventing the crossover of gases. The primary role of PEMs is to isolate gases and insulate electrons, allowing protons (H^+) to be transferred from the anode to the cathode, where they recombine with reduced oxygen atoms (O_2^-) to form water [36, 37]. If oxygen atoms on the cathode are not fully reduced or react with hydrogen permeating from the anode, hydrogen peroxide (H_2O_2) can form, which then decomposes into corrosive peroxide radicals (•OOH) and hydroxyl radicals (•OH). Under high temperatures and pressures within the fuel cell, these generated radicals accelerate the degradation of polymer materials. Given these circumstances, PEMs must meet strict requirements to ensure high efficiency and durability of the device. An ideal PEM should have high proton conductivity, good mechanical strength, high thermal stability, chemical stability, and low cost [38, 39].

Beyond conducting protons, PEMs also prevent electron transfer and maintain gas separation, ensuring that protons reach the cathode where they combine with oxygen to form water. However, if oxygen does not fully reduce or reacts

with hydrogen crossing the membrane, it can generate hydrogen peroxide (H_2O_2). At high temperatures and pressures, H_2O_2 decomposes into highly reactive radicals (•OH and •OOH) that degrade the membrane material. Thus, PEMs must be highly durable and meet rigorous standards for chemical, thermal, and mechanical stability to ensure long-term fuel cell performance.

In practical applications, PEMs need to deliver not only exceptional performance but also cost-effectiveness. They should have proton conductivity above 100 mS/cm, excellent electrical insulation, and minimal gas permeability, with hydrogen leakage currents under 2 mA/cm^2. Additionally, they must remain stable under hydrolytic, thermal, and oxidative conditions while maintaining sufficient water content to support conductivity even at low humidity. Robust mechanical properties in the hydrated state are crucial for reliable membrane electrode assembly operation, and keeping production costs below \$20/m^2 is a key economic target. By meeting these stringent requirements, PEMs can ensure high efficiency, stability, and affordability in PEM fuel cell systems.

1.2.3.1 Proton Transport Mechanisms

Proton conductivity is a critical parameter for evaluating PEMs. To enhance proton transport within the membrane, it is essential to first understand the underlying transport mechanisms. As illustrated in Figure 1.5, proton transport in PEMs primarily occurs through two mechanisms: the hopping mechanism (also known as the Grotthuss mechanism) [40] and the vehicle mechanism [41].

In the hopping mechanism (see Figure 1.5a), proton transport is achieved through the breaking and forming of hydrogen bonds as protons move from one active site to another. Initially, protons generated at the anode via oxidation reactions combine with water molecules to form hydronium ions. When a new proton appears nearby, the hydronium ion becomes unstable, causing a hydrogen bond to break. This releases the proton, which then "hops" to a neighboring ion site, forming a new hydrogen bond. While water molecules serve as carriers for transient hydrogen bonding, this mechanism can still function under high-temperature, low-humidity conditions. In fact, even in anhydrous environments, protons can bind to active carriers such as $–SO_3H$, $–NH_2$, –COOH, and $–PO_3H$, migrating to another active site via the same bond-breaking and bond-forming processes [42].

In the vehicle mechanism (see Figure 1.5b), protons associate with water molecules to form hydrated hydrogen ions (e.g. H_3O^+ or $H_5O_2^+$) that diffuse as a

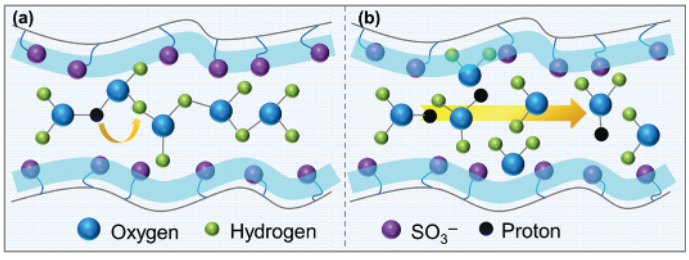

Figure 1.5 (a) Hopping mechanism and (b) vehicle mechanism.

single entity, without relying entirely on hydrogen bonds [43]. During this process, the proton and its associated water molecules move together, while unbound water molecules diffuse in the opposite direction. This results in a concentration gradient across the membrane, which facilitates the diffusion of both hydrated hydrogen ions and water molecules. For proton transport via the vehicle mechanism, the membrane's microstructure must contain continuous clusters of hydrated ions to provide pathways. However, under low-water-content conditions, the insufficient quantity and connectivity of these ion clusters hinder continuous proton transport, significantly reducing proton conductivity [44].

Proton transport is a complex process, typically occurring through both hopping and vehicle mechanisms. To enhance proton transport, three main approaches can be taken: increasing water content, optimizing proton transport channels, and increasing the number of proton carriers. Although increasing water content may appear to be the simplest method, doing so indiscriminately can lead to fragmented hydrophobic domains and decreased continuity of hydrophilic domains. This limitation not only reduces the extent of improvement but also compromises the mechanical stability of the membrane. Consequently, optimizing proton transport channels and increasing the number of proton carriers are more practical strategies.

i) **Optimizing Proton Transport Channels**: Improving proton transport channels can enhance the utilization of acid–water interactions, thereby increasing proton conductivity while maintaining appropriate water content [45]. Broadly speaking, proton transport channels refer to hydrophilic domains formed by acidic groups in the polymer chains. Under hydration, these acidic groups dissociate, generating proton carriers that migrate with the aid of hydrodynamic forces. In fact, proton transport channels can take various forms. When certain segments of a polymer's main chain, side chain, or functional groups exhibit differing hydrophilic and hydrophobic properties, microphase separation can occur, creating nanoscale interpenetrating regions [46, 47].

   However, traditional PEM materials like perfluorosulfonic acids or sulfonated hydrocarbon polymers tend to form "dead zones" that interrupt channel continuity, impeding smooth proton migration. Adding fillers—such as nanofibers, nanotubes, graphene, or metal-organic frameworks (MOFs)—can help eliminate these dead zones, transforming the convoluted channels into streamlined highways for proton transport.

   For example, Li et al. [48] developed bio-inspired caterpillar-like alumina fibers loaded with amine groups. These composite fibers were incorporated into sulfonated poly(ether sulfone) (SPES) to create a PEM that can achieve a proton conductivity of 0.263 S/cm at 80 °C and 100% relative humidity (RH), while also improving methanol permeability, thermal stability, and swelling resistance. Liu et al. [49] achieved similar results by synthesizing a ferricyanide coordination polymer that formed a proton-conducting paramagnetic composite

with phosphotungstic acid. By applying a magnetic field during the polymer casting process, they aligned the proton transport channels vertically, overcoming phosphotungstic acid loss. This design, supported by redox cycling of cyanide, produced a PEM with a maximum power density of 1107 mW/cm^2 and exceptional durability.

ii) **Increasing Proton Carriers**: Adding more proton carriers is another effective way to improve proton conductivity. Proton carriers generally fall into three categories: acidic, basic, and acid–base pair carriers. Acidic carriers, the earliest developed proton carriers, offer relatively high proton conductivity (10^{-2}–10^{-1} S/cm). They use acidic functional groups like –SO_3H or –PO_3H_2 to donate protons, thereby facilitating proton transport. However, excessive acidic groups can lead to excessive water absorption and swelling, which reduces acid concentration and dimensional stability, ultimately affecting the overall performance of the membrane [50]. Basic carriers, on the other hand, act as proton acceptors (e.g. –NH_2 or –NH^-), initially capturing free H^+ ions to form –NH_3^+. These then form intermediates such as –NH_3^+…OH^-…H^+, allowing H^+ ions to dissociate and transfer. Although basic carriers can transport protons, the strong electrostatic interactions between the basic groups and H^+ ions make proton dissociation more difficult, resulting in proton conductivities of less than 10^{-2} S/cm [51].

In contrast, acid–base pair carriers, a newer class of proton carriers, contain both acidic and basic groups. The electrostatic interactions between these groups facilitate proton hopping from acidic donor sites to basic acceptor sites. The electrostatic pairing also lowers the energy barrier for proton migration, thereby accelerating the process [52]. For instance, Sun et al. [53] synthesized double-shelled nanotubes with a carboxylate inner shell and an imidazole outer shell, which were then incorporated into sulfonated poly(ether ether ketone) (SPEEK) membranes. The imidazole outer shell formed acid–base pairs with both the inner shell and the SPEEK matrix, significantly enhancing proton hopping. The resulting membrane exhibited a proton conductivity of 0.336 S/cm at 80 °C and 100% RH, twice that of the original SPEEK membrane.

Similarly, Chen's team [54] combined sulfonic acid–functionalized graphitic carbon nitride nanosheets with sulfonated aromatic polymers. The acid–base pairs between the nanosheets and the matrix promoted sulfonate group dissociation and hydrogen-bond network formation. This "zipper-like" interface interaction induced phase separation and created long-range ionic pathways, resulting in excellent fuel cell performance of 717 mW/cm at 80 °C and 100% RH. Qu et al. [55] developed an acid–base composite membrane made from a carboxyl-containing polyimide and a basic polybenzimidazole for high-temperature PEM applications. Through electrostatic interactions and a continuous hydrogen-bond network, this membrane exhibited improved proton conductivity and enhanced phosphoric acid retention.

1.2.3.2 Classification of PEM

PEMs are a critical component of PEMFCs, directly determining the fuel cell performance. Consequently, PEMs must meet the following criteria [56, 57]:

1) High proton conductivity without electron conduction.
2) Excellent mechanical strength and dimensional stability, maintaining integrity under operational conditions.
3) Outstanding chemical and thermal stability, resisting degradation in harsh environments.
4) Low fuel crossover, effectively blocking reactants.
5) Low cost.

PEMs can be broadly categorized into homogeneous membranes and composite membranes based on their composition.

i) **Homogeneous Membranes**: Homogeneous membranes consist of a single type of material and can be further divided into fully fluorinated, partially fluorinated, and nonfluorinated membranes based on their polymer fluorine content. Nafion, the most common fully fluorinated sulfonic acid membrane, has a structure as shown in Figure 1.6a. Its hydrophobic PTFE backbone provides mechanical strength, while the hydrophilic side chains, terminated with sulfonic acid groups, offer proton transport sites. The distinct hydrophilic–hydrophobic nature of its main and side chains leads to phase separation in the microstructure, forming proton transport channels approximately 5–10 nm in diameter. High sulfonic acid group content endows Nafion with excellent proton conductivity, exceeding 100 mS/cm at 80 °C [59]. Thanks to its PTFE backbone, Nafion also boasts good mechanical, chemical, and thermal stability. However, Nafion's performance is highly sensitive to temperature and water content. Its low glass transition temperature limits its operating temperature to

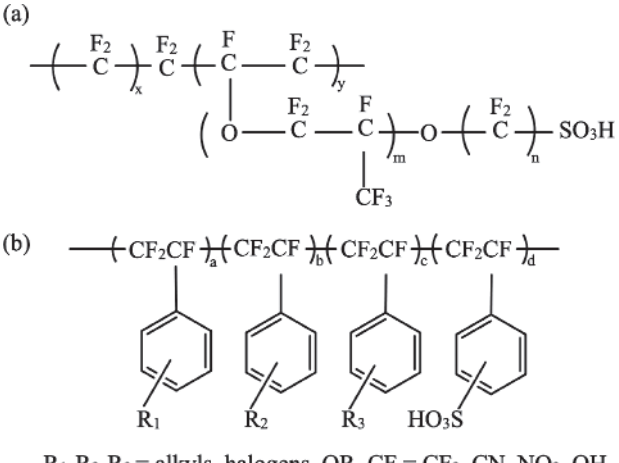

Figure 1.6 Structural formula of (a) Nafion and (b) BAM-3G. Source: Adapted from Basura et al. [58].

below 80 °C, and its proton conductivity drops significantly under low-humidity conditions due to reduced phase separation. Additionally, its high cost and significant fuel crossover impede further application [60–62].

To lower costs and simplify fabrication, researchers have increasingly turned to non-perfluorinated sulfonic acid PEMs. Partially fluorinated sulfonic acid PEMs are one example. These materials are similar to fully fluorinated membranes, with PTFE or polyvinylidene fluoride (PVDF) backbones and non-fluorinated aromatic groups in the side chains. For instance, the BAM-3G series PEMs from Canada's Ballard Power Systems are synthesized by copolymerizing substituted trifluorostyrenes and sulfonated trifluorostyrenes, as shown in Figure 1.6b. These membranes feature low sulfonic acid content, high efficiency, and extended lifetimes (up to 15,000 hours for single cells) at a fraction of Nafion's cost, making them more accessible [58].

Another major category of homogeneous membranes is non-fluorinated sulfonic acid PEMs, which mainly include sulfonated aromatic polymers such as SPEEK, SPES, sulfonated polyimides, and sulfonated polybenzimidazoles [63–66]. Compared to aliphatic polymers, these polymers contain a higher proportion of rigid aromatic groups in their molecular backbones, providing the membranes with good mechanical properties and thermal stability. They can easily be sulfonated to introduce sulfonic acid groups, are derived from widely available materials, and have relatively simple preparation methods. Moreover, the absence of costly fluorination steps significantly reduces their production costs. However, due to shorter side chains, less-pronounced phase separation, and a lower sulfonic acid group content compared to perfluorosulfonic acid membranes, nonfluorinated sulfonic acid PEMs generally exhibit lower proton conductivity [67]. Additionally, they tend to have high humidity requirements and limited durability, which remain challenges to overcome.

ii) **Composite Membranes**: Whether fully fluorinated, partially fluorinated, or nonfluorinated sulfonic acid membranes, each type has its own strengths and weaknesses, making it difficult to find a homogeneous PEM that excels in all aspects. Modifying a homogeneous PEM—such as by incorporating fillers—can produce composite membranes that address these limitations. Composite membranes offer unique advantages over homogeneous membranes, including the ability to integrate the benefits of the fillers and to tailor performance improvements for specific needs. Depending on the nature of the filler, modification methods can be categorized as either organic–inorganic or organic–organic approaches.

a) **Organic–Inorganic Modification**: Introducing inorganic components can effectively enhance proton conductivity, particularly for sulfonated polymers under low-humidity conditions. Common inorganic fillers include silica [68], heteropoly acids [69], carbon materials [34], and MOFs [70]. These fillers can improve water retention, dimensional stability, mechanical strength, and methanol permeability to varying degrees. Inorganic fillers can be introduced by methods such as doping, sol-gel processes, or in situ synthesis.

For example, Yan et al. [71] prepared sulfonated mesoporous silica frameworks with controlled channel sizes of approximately 0.5 nm, slightly larger than the diameter of H_3O+ ions (0.28 nm) and slightly smaller than methanol molecules (0.4 nm). These molecular sieve-like membranes, when combined with Nafion, showed methanol permeability three orders of magnitude lower than Nafion. Pei et al. [72] introduced CeO_2-based core–shell micro/nanostructures rich in tourmaline into perfluorosulfonic resin, resulting in a composite membrane with excellent proton conductivity and chemical stability. At 80 °C and 100% RH, the composite membrane achieved a maximum power density of 1006 mW/cm^2, higher than Nafion's 906 mW/cm^2 under the same conditions. Additionally, CeO_2 helps scavenge hydroxyl radicals, slowing degradation and improving the membrane's durability.

b) **Organic–Organic Modification**: Organic modifications involve incorporating functional organic materials into the polymer matrix. This approach can compensate for the inherent shortcomings of the polymer matrix while selectively enhancing specific properties. Organic fillers can be divided into small organic molecules and macromolecular organic substances [73–75].

Small organic molecules include covalent-organic frameworks, hydrogen-bonded organic frameworks, and ionic liquids (ILs), while macromolecular organic fillers include PVDF, polyvinyl alcohol, and sulfonated polymers. These fillers interact with the polymer matrix through various mechanisms, supplementing missing functions and enhancing existing performance. For instance, Sun's group [41] hydrogen-bonded Nafion with polyvinyl alcohol and then post-modified it with 4-carboxybenzaldehyde to produce a repairable PEM. This PEM demonstrated superior mechanical stability (with a tensile strength of 20.3 MPa and strain of 380%), improved proton conductivity (0.11 S/cm at 80 °C, 1.2 times that of Nafion), and resistance to methanol permeation. Under methanol fuel cell conditions, the membrane could self-heal mechanical damage up to tens of microns in size.

Zhao and co-workers [76] embedded Nafion nanofibers into a polybenzimidazole matrix to create a Nafion/polybenzimidazole composite membrane. The polybenzimidazole provided high ion selectivity, while the fibrous Nafion ensured high proton conductivity and low cost. Compared to Nafion 212, the composite membrane, with only 40 wt% Nafion, exhibited a 58-fold reduction in vanadium crossover and achieved 99.8% coulombic efficiency and 80.0% energy efficiency at a high current density of 210 mA/cm^2 in vanadium redox flow batteries.

References

1 Mohideen, M.M., Subramanian, B., Sun, J. et al. (2023). Techno-economic analysis of different shades of renewable and non-renewable energy-based hydrogen for fuel cell electric vehicles. *Renewable and Sustainable Energy Reviews* 174: 113153.

2 Cano, Z.P., Banham, D., Ye, S. et al. (2018). Batteries and fuel cells for emerging electric vehicle markets. *Nature Energy* 3: 279–289.

3 Pollet, B.G., Kocha, S.S., and Staffell, I. (2019). Current status of automotive fuel cells for sustainable transport. *Current Opinion in Electrochemistry* 16: 90–95.

4 Mohideen, M.M., Ramakrishna, S., Prabu, S. et al. (2021). Advancing green energy solution with the impetus of COVID-19 pandemic. *Journal of Energy Chemistry* 59: 688–705.

5 Staffell, I., Scamman, D., Abad, A.V. et al. (2019). The role of hydrogen and fuel cells in the global energy system. *Energy & Environmental Science* 12: 463–491.

6 Mohideen, M.M., Liu, Y., and Ramakrishna, S. (2020). Recent progress of carbon dots and carbon nanotubes applied in oxygen reduction reaction of fuel cell for transportation. *Applied Energy* 257: 114027.

7 Banham, D., Zou, J., Mukerjee, S. et al. (2021). Ultralow platinum loading proton exchange membrane fuel cells: performance losses and solutions. *Journal of Power Sources* 490: 229515.

8 Mohideen, M.M., Radhamani, A.V., Ramakrishna, S. et al. (2022). Recent insights on iron based nanostructured electrocatalyst and current status of proton exchange membrane fuel cell for sustainable transport. *Journal of Energy Chemistry* 69: 466–489.

9 Wang, Y. (2018). A brief history and application of electrospinning technology development. *China Synthetic Fiber Industry* 41 (04): 52–57.

10 Liu, Y., Ding, H., Ding, D. et al. (2018). Overview of electrospinning preparation of proton exchange membrane fuel cell catalyst layer. *Journal of Electrochemistry* 24 (06): 639–654.

11 Lv, Y., Sang, X., Tian, Z. et al. (2022). Electrospun hydroxyapatite loaded L-polylactic acid aligned nanofibrous membrane patch for rotator cuff repair. *International Journal of Biological Macromolecules* 217: 180–187.

12 Wang, Y., Chen, K.S., Mishler, J. et al. (2011). A review of polymer electrolyte membrane fuel cells: technology, applications, and needs on fundamental research. *Applied Energy* 88 (4): 981–1007.

13 Larminie, J. and Dicks, A. (2003). *Fuel Cell Systems Explained*, 2e, 1–43. Antony Rowe Ltd: Chippenham.

14 Shui, J., Wang, M., Du, F. et al. (2015). N-doped carbon nanomaterials are durable catalysts for oxygen reduction reaction in acidic fuel cells. *Science Advances* 1 (1): e1400129.

15 Qin, C., Wang, J., Yang, D. et al. (2016). Proton exchange membrane fuel cell reversal: a review. *Catalysts* 6 (12): 197.

16 Tamura, T. and Kawakami, H. (2010). Aligned electrospun nanofiber composite membranes for fuel cell electrolytes. *Nano Letters* 10 (4): 1324–1328.

17 Fofana, D., Hamelin, J., and Bénard, P. (2013). Modelling and experimental validation of high performance low platinum multilayer cathode for polymer electrolyte membrane fuel cells (PEMFCs). *International Journal of Hydrogen Energy* 38 (24): 10050–10062.

18 Tian, Z.Q., Lim, S.H., Poh, C.K. et al. (2011). A highly order-structured membrane electrode assembly with vertically aligned carbon nanotubes for ultra-low pt loading PEM fuel cells. *Advanced Energy Materials* 1 (6): 1205–1214.

19 Manikandan, T. and Ramalingam, S. (2016). A review of optimization algorithms for the modeling of proton exchange membrane fuel cell. *Journal of Renewable and Sustainable Energy* 8 (3): 1103–1112.

20 Li, Y., Li, Q., Wang, H. et al. (2019). Recent progresses in oxygen reduction reaction electrocatalysts for electrochemical energy applications. *Electrochemical Energy Reviews* 2: 518–538.

21 Zhong, H.-X., Zhang, Y., and Zhang, X.-B. (2018). Superior oxygen reduction electrocatalyst: hollow porous spinel microsphere. *Chem* 4: 196–198.

22 Thompson, S.T., Wilson, A.R., Zelenay, P. et al. (2018). ElectroCat: DOE's approach to PGM-free catalyst and electrode R&D. *Solid State Ionics* 319: 68–76.

23 Wang, X., Li, Z., Qu, Y. et al. (2019). Review of metal catalysts for oxygen reduction reaction: from nanoscale engineering to atomic design. *Chem* 5: 1486–1511.

24 Primbs, M., Sun, Y., Roy, A. et al. (2020). Establishing reactivity descriptors for platinum group metal (PGM)-free Fe–N–C catalysts for PEM fuel cells. *Energy & Environmental Science* 13: 2480–2500.

25 Huang, Z.-F., Song, J., Dou, S. et al. (2019). Strategies to break the scaling relation toward enhanced oxygen electrocatalysis. *Matter* 1: 1494–1518.

26 Ganesan, A. and Narayanasamy, M. (2019). Ultra-low loading of platinum in proton exchange membrane-based fuel cells: a brief review. *Materials for Renewable and Sustainable Energy* 8: 18.

27 Okonkwo, P.C. and Otor, C. (2021). A review of gas diffusion layer properties and water management in proton exchange membrane fuel cell system. *International Journal of Energy Research* 45 (3): 3780–3800.

28 Omrani, R. and Shabani, B. (2017). Gas diffusion layer modifications and treatments for improving the performance of proton exchange membrane fuel cells and electrolysers: a review. *International Journal of Hydrogen Energy* 42 (47): 28515–28536.

29 Cindrella, L., Kannan, A.M., Lin, J.F. et al. (2009). Gas diffusion layer for proton exchange membrane fuel cells—a review. *Journal of Power Sources* 194 (1): 146–160.

30 Athanasaki, G., Jayakumar, A., and Kannan, A.M. (2023). Gas diffusion layers for PEM fuel cells: materials, properties and manufacturing—a review. *International Journal of Hydrogen Energy* 48 (6): 2294–2313.

31 Jayakumar, A., Sethu, S.P., Ramos, M. et al. (2015). A technical review on gas diffusion, mechanism and medium of PEM fuel cell. *Ionics* 21: 1–18.

32 Zhang, G., Qu, Z., Tao, W.Q. et al. (2022). Porous flow field for next-generation proton exchange membrane fuel cells: materials, characterization, design, and challenges. *Chemical Reviews* 123 (3): 989–1039.

33 Ji, M. and Wei, Z. (2009). A review of water management in polymer electrolyte membrane fuel cells. *Energies* 2 (4): 1057–1106.

34 Madheswaran, D.K., Thangavelu, P., Krishna, R. et al. (2023). Carbon-based materials in proton exchange membrane fuel cells: a critical review on performance and application. *Carbon Letters* 33 (6): 1495–1518.

35 Zhang, B., Hua, Y., and Gao, Z. (2022). Strategies to optimize water management in anion exchange membrane fuel cells. *Journal of Power Sources* 525: 231141.

36 Wang, Y., Pang, Y., Xu, H. et al. (2022). PEM fuel cell and electrolysis cell technologies and hydrogen infrastructure development—a review. *Energy & Environmental Science* 15 (6): 2288–2328.

37 Qasem, N.A. (2024). A recent overview of proton exchange membrane fuel cells: fundamentals, applications, and advances. *Applied Thermal Engineering* 252: 123746.

38 Xie, Z., Wang, J., Zhao, G. et al. (2024). A review on durability of key components of PEM fuel cells. *Catalysis Science & Technology* 252.

39 Zhang, K., Liang, X., Wang, L. et al. (2022). Status and perspectives of key materials for PEM electrolyzer. *Nano Research Energy* 1 (3): e9120032.

40 Li, J., Lou, J., Wang, Z. et al. (2020). Facilitating proton transport with enhanced water conservation membranes for direct methanol fuel cells. *ACS Sustainable Chemistry & Engineering* 8 (15): 5880–5890.

41 Li, Y., Liang, L., Liu, C. et al. (2018). Self-healing proton-exchange membranes composed of nafion–poly(vinyl alcohol) complexes for durable direct methanol fuel cells. *Advanced Materials* 30 (25): 1707146.

42 Oka, T., Oshima, A., and Washio, M. (2024). Free volume study of sulfonated FEP proton exchange membrane. *Radiation Physics and Chemistry* 215: 111364.

43 Xu, G., Ke, A., Xu, G. et al. (2024). Enabling high-temperature application of Nafion membrane via imitating ionic clusters in proton conduction channels. *International Journal of Hydrogen Energy* 56: 330–337.

44 Guan, P., Lei, J., Liu, X. et al. (2022). Origins of water state and ionic cluster morphology for high proton conductivity of short side-chain perfluorinated sulfonic acid membranes. *Chemistry of Materials* 34 (17): 7845–7857.

45 Guan, P., Zou, Y., Zhang, M. et al. (2024). High-temperature low-humidity proton exchange membrane with "stream-reservoir" ionic channels for high-power-density fuel cells. Science. *Advances* 9 (17): eadh1386.

46 Golubenko, D.V., Shaydullin, R.R., and Yaroslavtsev, A.B. (2019). Improving the conductivity and permselectivity of ion-exchange membranes by introduction of inorganic oxide nanoparticles: impact of acid–base properties. *Colloid and Polymer Science* 297 (5): 741–748.

47 Chen, L., Ren, Y., Fan, F. et al. (2023). Artificial frameworks towards ion-channel construction in proton exchange membranes. *Journal of Power Sources* 574: 233081.

48 Li, L., Liu, X., Guo, Y. et al. (2022). Reasonable construction of proton conducting channel via biomimetic caterpillar-like alumina fiber to improve the properties of its composite proton exchange membrane. *International Journal of Hydrogen Energy* 47 (69): 29915–29924.

49 Liu, X., Li, Y., Xue, J. et al. (2019). Magnetic field alignment of stable proton-conducting channels in an electrolyte membrane. *Nature Communications* 10 (1): 842.

50 Wang, G., Kang, J., Yang, S. et al. (2024). Influence of structure construction on water uptake, swelling, and oxidation stability of proton exchange membranes. *International Journal of Hydrogen Energy* 50: 279–311.

51 He, Y., Wang, J., Zhang, H. et al. (2014). Polydopamine-modified graphene oxide nanocomposite membrane for proton exchange membrane fuel cell under anhydrous conditions. *Journal of Materials Chemistry A* 2 (25): 9548–9558.

52 Li, G., Shen, R., Hu, S. et al. (2022). Norbornene-based acid–base blended polymer membranes with low ion exchange capacity for proton exchange membrane fuel cell. *Advanced Composites and Hybrid Materials* 5 (3): 2131–2137.

53 Sun, X., Zhang, T., Liu, X. et al. (2020). Multi-functionalized acid-base double-shell nanotubes are incorporated into the proton exchange membrane to cope with low humidity conditions. *International Journal of Hydrogen Energy* 45 (55): 30673–30688.

54 Lu, Y., Liu, Y., Li, N. et al. (2020). Sulfonated graphitic carbon nitride nanosheets as proton conductor for constructing long-range ionic channels proton exchange membrane. *Journal of Membrane Science* 601: 117908.

55 Qu, E., Cheng, G., Xiao, M. et al. (2023). Composite membranes consisting of acidic carboxyl-containing polyimide and basic polybenzimidazole for high-temperature proton exchange membrane fuel cells. *Journal of Materials Chemistry A* 11 (24): 12885–12895.

56 Zeng, L., Lu, X., Yuan, C. et al. (2024). Self-enhancement of perfluorinated sulfonic acid proton exchange membrane with its own nanofibers. *Advanced Materials* 36: 2305711.

57 Xin, Z., Yanyi, Z., and Xiaobing, W. (2023). Research on testing and evaluation technology of proton exchange membrane for fuel cell. *Energy Reports* 10: 1943–1950.

58 Basura, V.I., Chuy, C., Beattie, P.D. et al. (2001). Effect of equivalent weight on electrochemical mass transport properties of oxygen in proton exchange membranes based on sulfonated α,β,β-trifluorostyrene (BAM®) and sulfonated styrene-(ethylene-butylene)-styrene triblock (DAIS-analytical) copolymers. *Journal of Electroanalytical Chemistry* 501 (1): 77–88.

59 Pourzare, K., Mansourpanah, Y., Farhadi, S. et al. (2020). Improving the efficiency of Nafion-based proton exchange membranes embedded with magnetically aligned silica-coated Co_3O_4 nanoparticles. *Solid State Ionics* 351: 115343.

60 Teixeira, F.C., De Sá, A.I., Teixeira, A.P.S. et al. (2019). Nafion phosphonic acid composite membranes for proton exchange membranes fuel cells. *Applied Surface Science* 487: 889–897.

61 Li, J., Xu, G., Cai, W. et al. (2018). Non-destructive modification on Nafion membrane via in-situ inserting of sheared graphene oxide for direct methanol fuel cell applications. *Electrochimica Acta* 282: 362–368.

62 Wang, H., Li, X., Zhuang, X. et al. (2017). Modification of Nafion membrane with biofunctional SiO_2 nanofiber for proton exchange membrane fuel cells. *Journal of Power Sources* 340: 201–209.

63 Li, J., Cui, N., Liu, D. et al. (2024). SPEEK-co-PEK-x proton exchange membranes with controllable sulfonation degree for proton exchange membrane fuel cells. *International Journal of Hydrogen Energy* 50: 606–617.

64 Justin Jose Sheela, A.S., Moorthy, S., Maria Mahimai, B. et al. (2023). Sulfonated poly ether sulfone membrane reinforced with bismuth-based organic and inorganic additives for fuel cells. *ACS Omega* 8 (30): 27510–27518.

65 Balasubramanian, A., Gunasekaran, M., and Kannan, T. (2022). Photo crosslinked stilbene-containing sulfonated polyimide membranes as proton exchange membranes in fuel cell. *European Polymer Journal* 176: 111418.

66 Liang, J., Ge, J., Wu, K. et al. (2020). Sulfonated polyaryletherketone with pendant benzimidazole groups for proton exchange membranes. *Journal of Membrane Science* 597: 117626.

67 Liu, L., Wang, C., He, Z. et al. (2021). Bi-functional side chain architecture tuned amphoteric ion exchange membranes for high-performance vanadium redox flow batteries. *Journal of Membrane Science* 624: 119118.

68 Zheng, C., Xie, N., Liu, X. et al. (2024). Durability improvement of proton exchange membrane fuel cells by doping silica–ferrocyanide antioxidant. *Journal of Membrane Science* 690: 122195.

69 Ryu, G.Y., Jae, H., Kim, K.J. et al. (2023). Hollow heteropoly acid-functionalized ZIF composite membrane for proton exchange membrane fuel cells. *ACS Applied Energy Materials* 6 (8): 4283–4296.

70 Devrim, Y. and Colpan, C.O. (2024). Assessment of polybenzimidazole/MOF composite membranes for the improvement of high-temperature PEM fuel cell performance. *International Journal of Hydrogen Energy* 58: 470–478.

71 Yan, X., Li, H., Lin, C. et al. (2020). An inorganic-framework proton exchange membrane for direct methanol fuel cells with increased energy density. *Sustainable Energy & Fuels* 4 (2): 772–778.

72 Pei, S., Xu, K., Xu, X. et al. (2023). CeO_2 stabilized by tourmaline as a novel inorganic filler to simultaneously increase the conductivity and durability of proton exchange membranes. *Inorganic Chemistry Frontiers* 10 (11): 3335–3344.

73 Yang, X., Zhu, H., Jiang, F. et al. (2020). Notably enhanced proton conductivity by thermally-induced phase-separation transition of Nafion/Poly (vinylidene fluoride) blend membranes. *Journal of Power Sources* 473: 228586.

74 Xu, X.Q., Cao, L.H., Yang, Y. et al. (2021). Hybrid Nafion membranes of ionic hydrogen-bonded organic framework materials for proton conduction and PEMFC applications. *ACS Applied Materials & Interfaces* 13 (47): 56566–56574.

75 Xu, F., Han, Y., Huang, K. et al. (2024). Enhanced performance of high-temperature proton exchange membranes via polyfluorene cross-linked zwitterionic liquid. *Journal of Membrane Science* 694: 122434.

76 Wan, Y.H., Sun, J., Jian, Q.P. et al. (2022). A Nafion/polybenzimidazole composite membrane with consecutive proton-conducting pathways for aqueous redox flow batteries. *Journal of Materials Chemistry A* 10 (24): 13021–13030.